# Properties of electron pressure anisotropy in the extended electron diffusion region

A. Divin(1,2), V. Semenov(1), S. Markidis (3), G. Lapenta(4)
J. Deca(5), V. Olshevsky(4), D. Korovinskiy(1)
[1]St. Petersburg State University
[2]IRF Uppsala, Sweden
[3]KTH Royal Institute of Technology
[4]KU Leuven
[5]Laboratory for Atmospheric and Space Physics (LASP), Boulder, USA

August 10 2015 - Nordita

# Outline

- Do we have clear understanding of c'less 2D EDR?
- Diffusion in antiparallel 2D collisionless reconnection (nearly textbook task)
- Ohm's law terms across diffusion region
- Inner and external EDR
- Electron pressure anisotropy in the inner and external EDR

# DR in collisionless reconnection

- Diffusion in antiparallel collisionless reconnection.

$$\mathbf{E} + \mathbf{V}_e \times \mathbf{B} = -\frac{1}{n_e e}\nabla \cdot \mathbf{P}_e - \frac{m_e}{e}\frac{d\mathbf{v}_e}{dt} + \eta \mathbf{j}$$

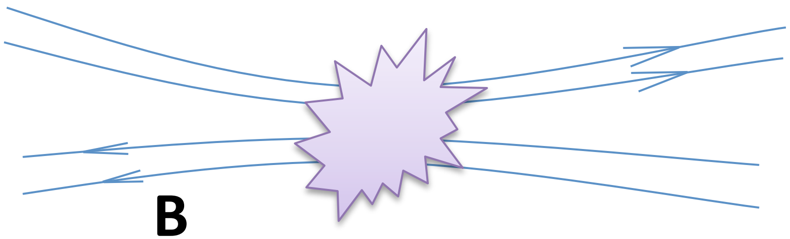


- Unmagnetized electrons: meandering motions.
- Several models for electron pressure closure near X-line were developed previously, however…

# EDR: Ohm's law

$P_{yz}$

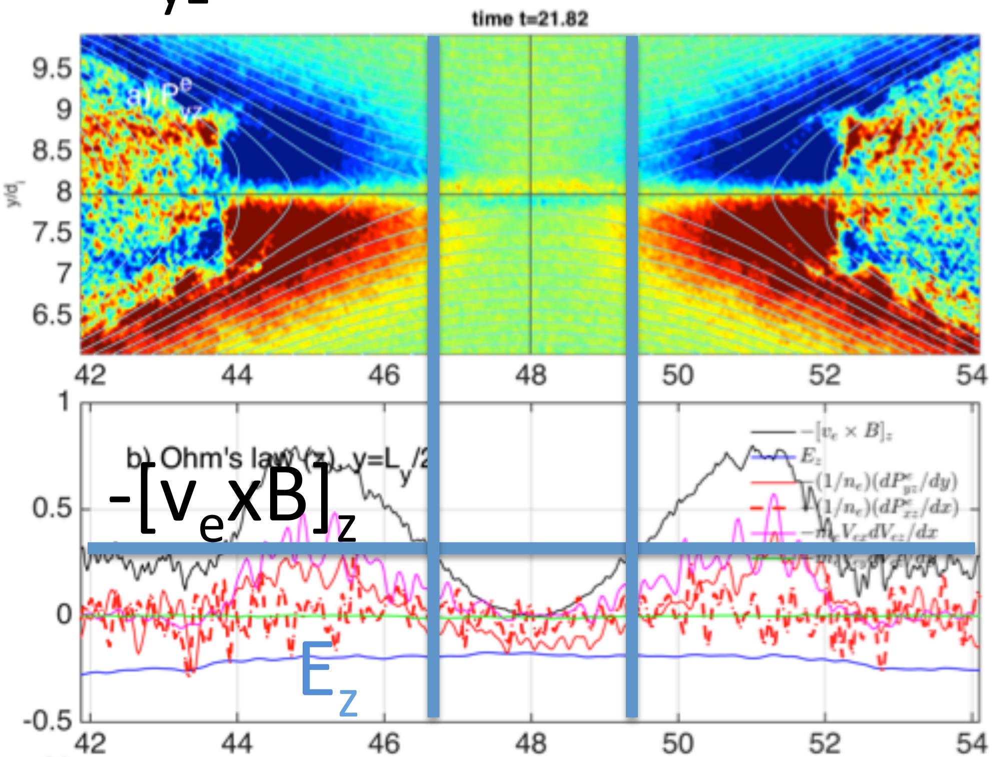


Anisotropy of electron pressure (**mostly $P_{eyz}$**) supports $E_z$ near X-point)

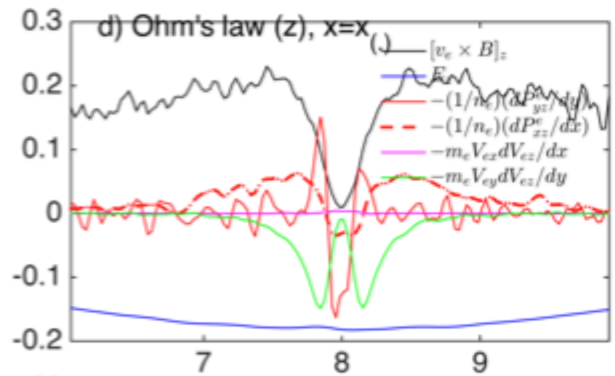


'classical' EDR: $|V_e xB|<|Ez|$

'extended' EDR: $|V_e xB|>|Ez|$

# Simulation

- Implicit particle-in-cell (PIC) electromagnetic parallel code [Markidis, 2010] iPIC3D
- Harris equilibrium + X-point initial perturbation
- $Lx=96d_i$ , $Ly=16d_i$ (3456x576 grid cells)

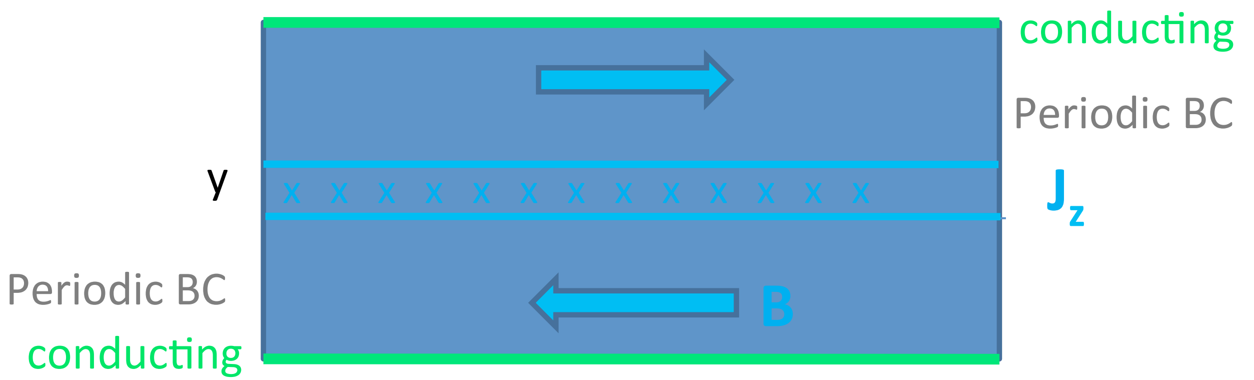


- Mass ratio $m_i/m_e=256$, $c/v_A=103$, $T_i/T_e=5$
- 2D plane: X-Y; current direction: Z

# What do we understand now?

$J_{ez}$

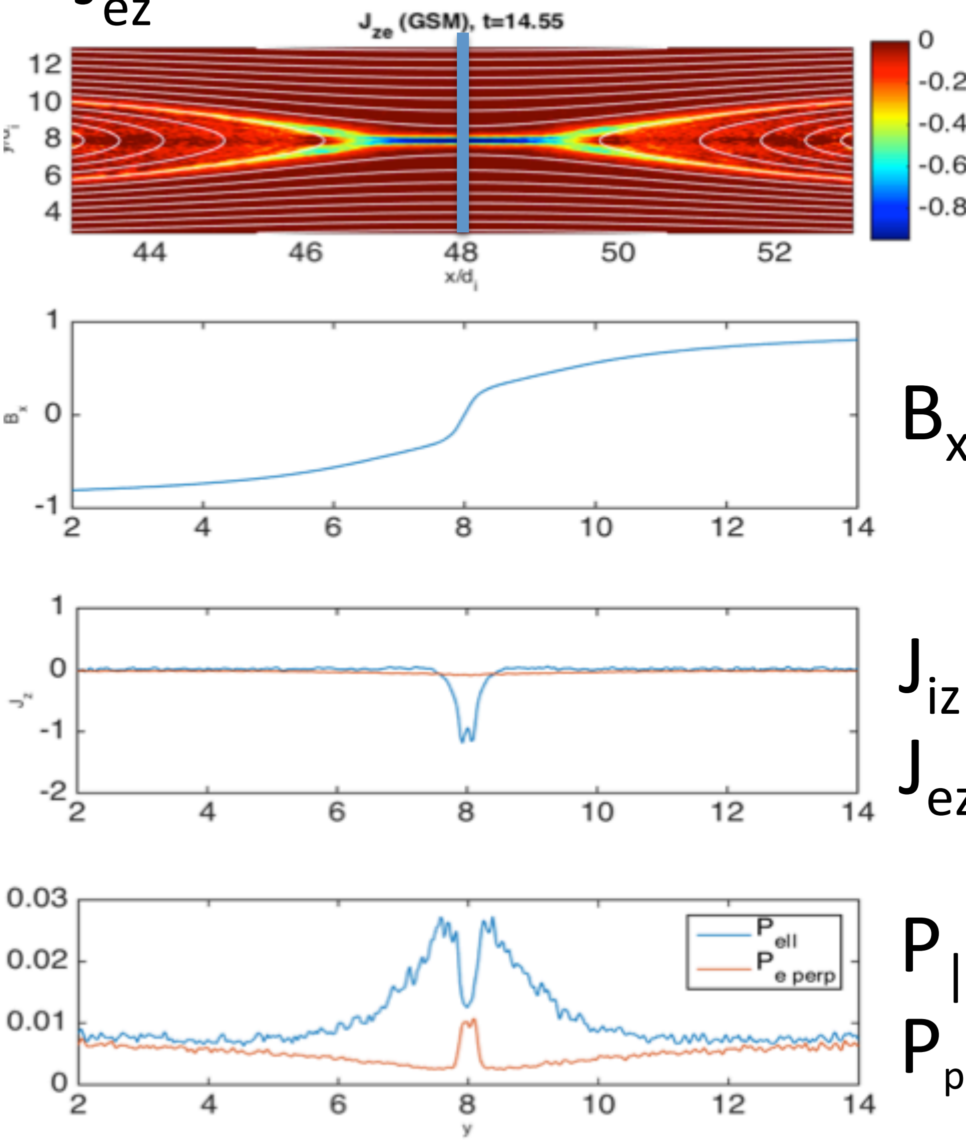


$B_x$

$J_{iz}$

$J_{ez}$

$P_{||}$

$P_{perp}$

- Strong $J_{ez}$ inside the EDR, weak but extended $J_{iz}$ inside IDR
- Bx reduces gradually ~3 times near the EDR edge
- Electrons are magnetized above the EDR edge
- Reduction of |B|, hence $P_{||}$ anisotropy develops, CGL invariants.

# Pressure anisotropy

Maxwellian, isotropic:

$$f(\mathbf{v}) = \left(\frac{m}{2\pi kT}\right)^{\frac{3}{2}} \exp\left\{-\frac{m\mathbf{v}^2}{2kT}\right\}$$

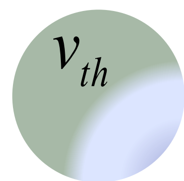


$$\hat{\mathrm{P}} = \mathrm{I}p = \begin{pmatrix} nkT & & 0 \\ & nkT & \\ 0 & & nkT \end{pmatrix}$$

$$f(\mathbf{v}) \sim \exp\left\{-\frac{\mathbf{v}^2}{v_{th\|}^2} - \frac{\mathbf{v}^2}{v_{th\perp}^2}\right\}$$

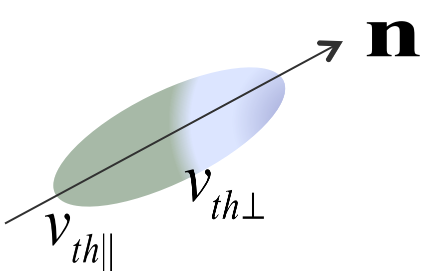


$$\hat{\mathrm{P}} = p_{\|}\mathbf{nn} + p_{\perp}(\mathbf{I} - \mathbf{nn})$$

$$f_N(x_1, x_2, \ldots, x_N) = \frac{1}{(2\pi)^{\frac{N}{2}}(det\Sigma)^{\frac{1}{2}}} \exp\left(-\frac{1}{2}(\mathbf{x}-\mu)^{\mathrm{T}}\boldsymbol{\Sigma}^{-1}(\mathbf{x}-\mu)\right)$$

$\hat{\mathrm{P}} = mn\Sigma$, arbitrary

$\Sigma$ - covariance matrix

$\mu$ - mean <**x**>

# Electron pressure anisotropy

Gyrotropic part
$P_{yz}=(P_{e||}-P_{epr})b_y b_z$

CGL invariant $\dfrac{P_{e\perp}}{nB^{\gamma_\perp -1}}$

CGL invariant $\dfrac{P_{e\|}B^{\gamma_\| -1}}{n^{\gamma_\|}}$

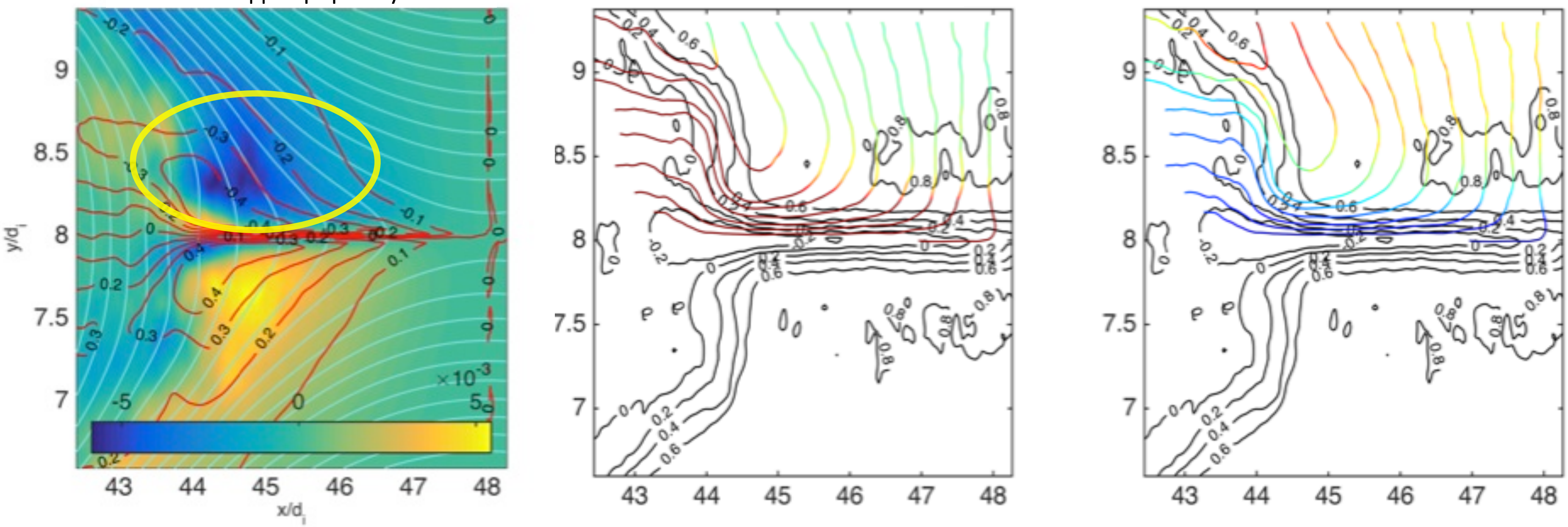


Electron Pyz component is well described by the gyrotropic expression there!

The parallel and perpendicular CGL invariants are conserved well in the inflow region

# EDR d.f.'s near the X-line

$f_e(v_x,v_y)$ $f_e(v_x,v_z)$ $f_e(v_z,v_y)$

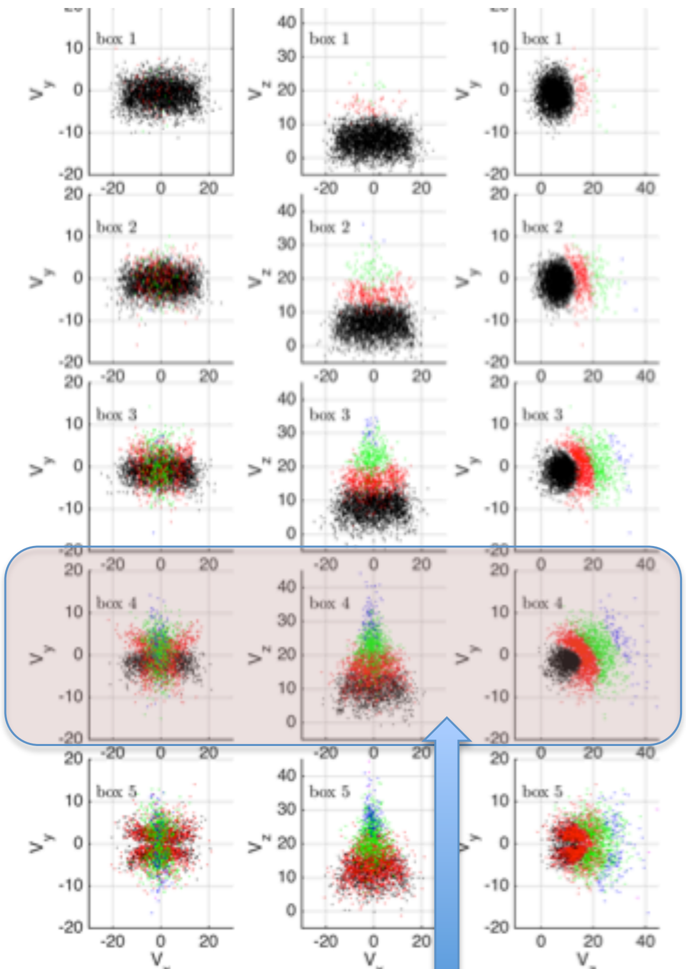


$P_{yz}$

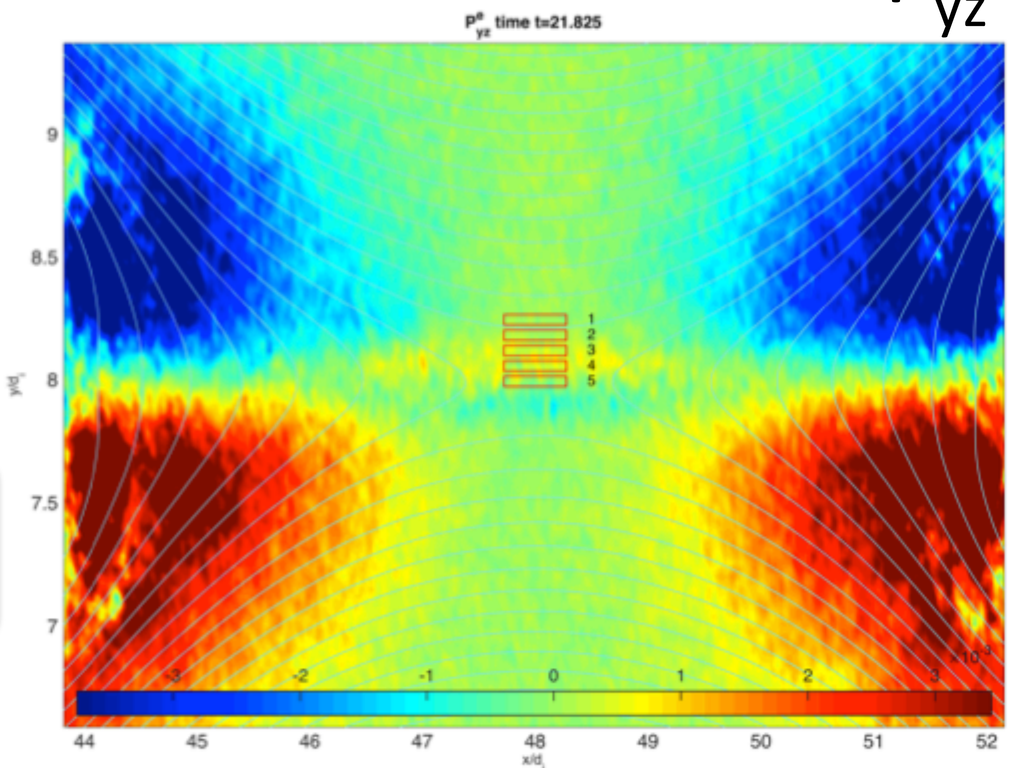


A number of meandering oscillation crossings is shown color

# EDR d.f.'s, edge

$f_e(v_x,v_y)$ $f_e(v_x,v_z)$ $f_e(v_z,v_y)$

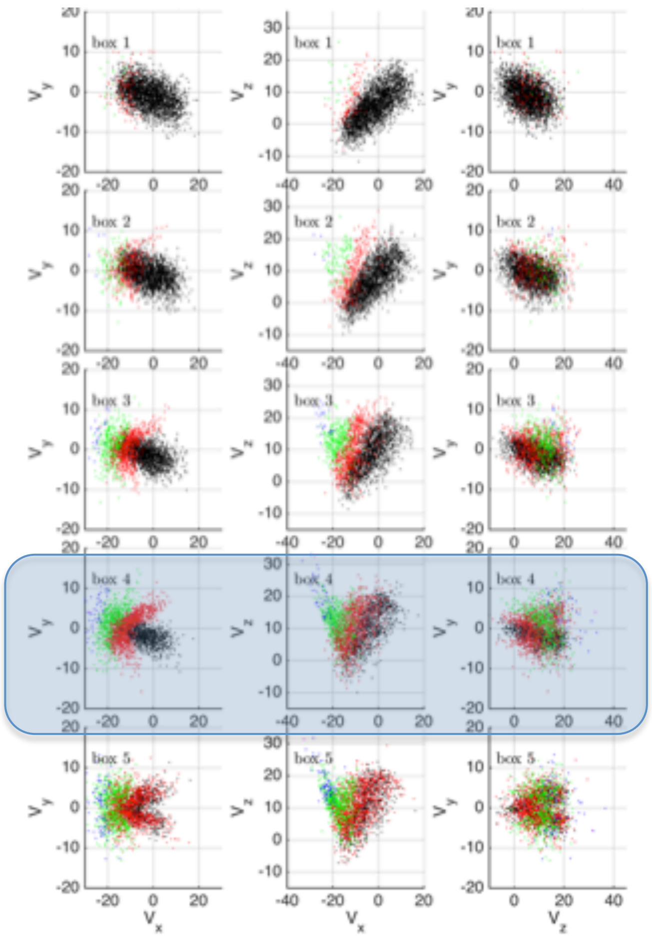


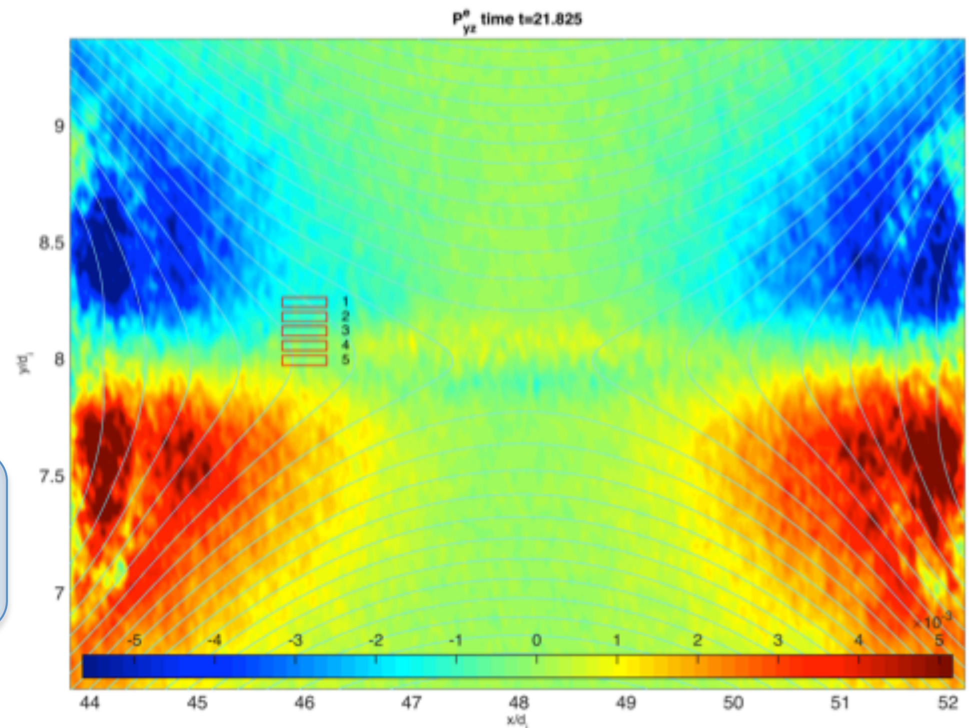


Distribution functions are rather 3D and structured, but what if we rotate…

# EDR , rotated

$f_e(v_x,v_y)$ $f_e(v_x,v_z)$ $f_e(v_z,v_y)$

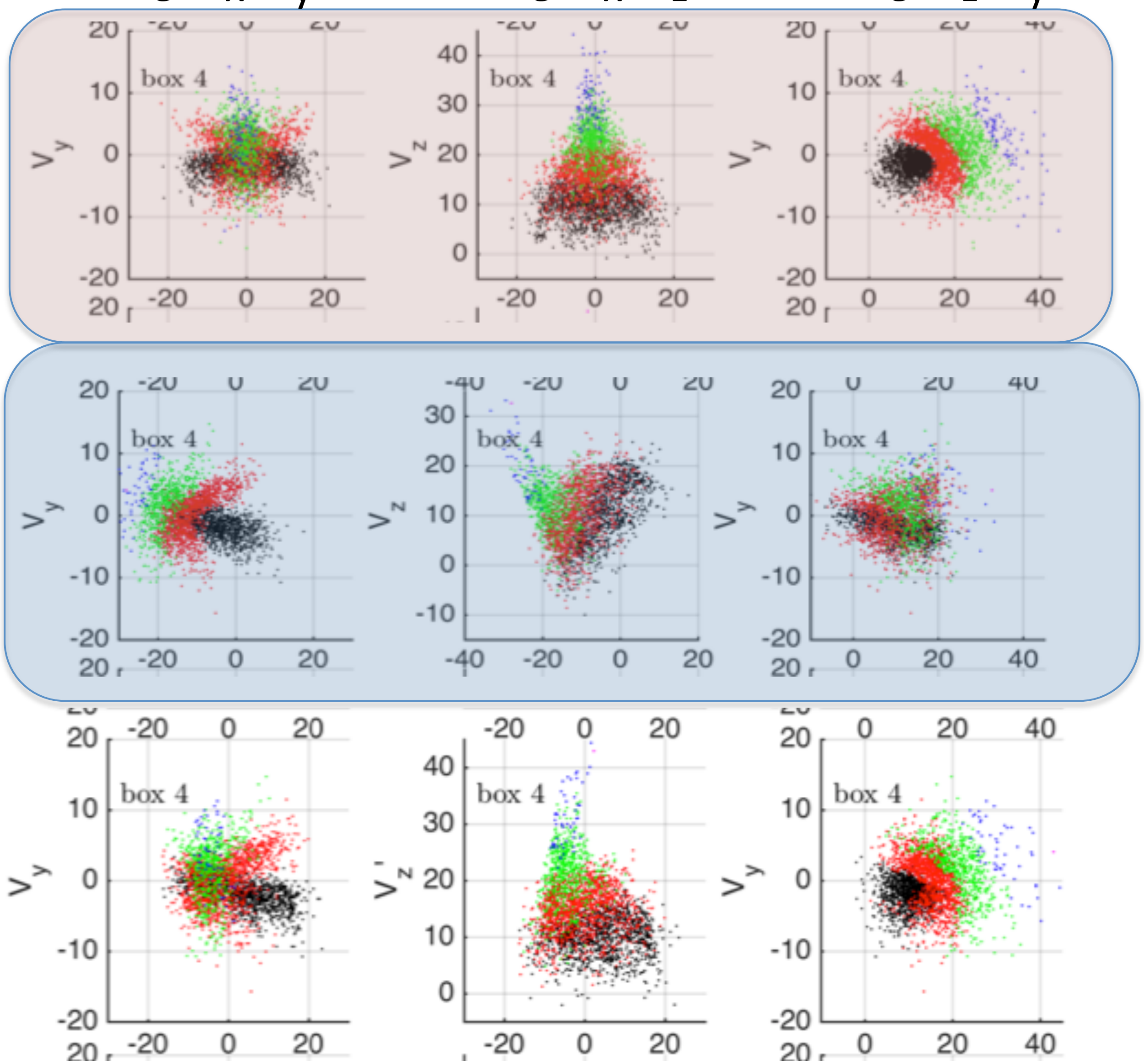


X-line vicinity

EDR downstream

**Rotated EDR downstream**

# Rotated Pyz component

$P_{xy}$

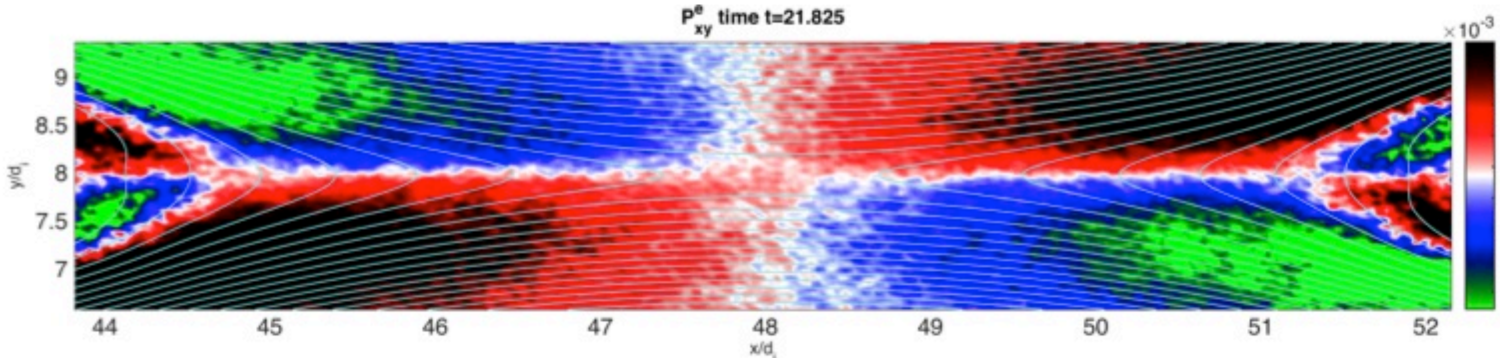


$P_{yz}$

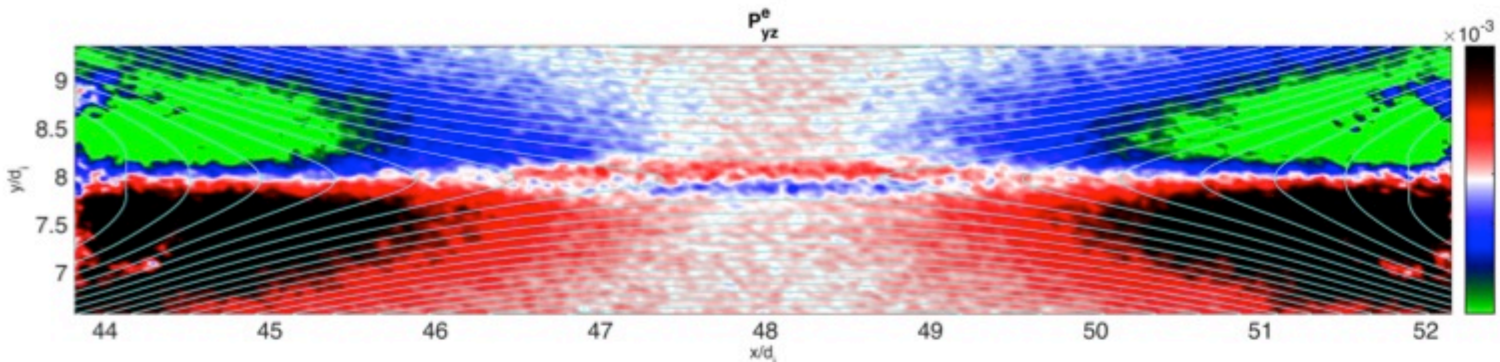


Electron distribution functions $f(v_y,v_z)$ in the rotated frame are similar to that right at X-line

Rotating the pressure tensor around Y (vertical axis) provides $P'_{yz} = P_{yz}\cos\alpha + P_{xy}\sin\alpha$

# Rotated Pyz': invariant

P'$_{yz}$

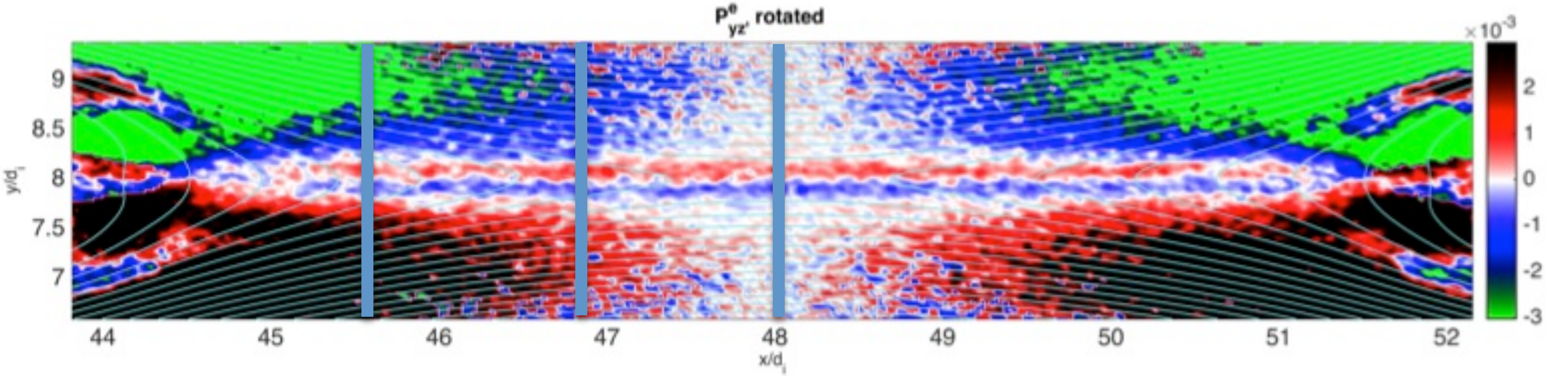


- *The profile of $P'_{yz}(y)$ is nearly invariant along x*
- By definition $P'_{yz}(y)=P_{yz}(y)$ for $x=x_{(.)}$
- By substituting $P'_{yz}(y)=P_{yz}(x_{(.)},y)$ and $\frac{P'_{yz}}{\cos\alpha} - P_{xy}\tan\alpha = P_{yz}$ the component Pyz is found:

$$P_{yz}(x,y) = \frac{P^{(0)}_{yz}(y)}{\cos\alpha} - P_{xy}(x,y)\frac{v_x}{v_z},\ \alpha = \text{atan}\ \frac{v_x}{v_z}$$

# $P_{yz}$: composite model

$$P_{yz}(x,y) = \frac{P^{(0)}_{yz}(y)}{\cos\alpha} - P_{xy}(x,y)\frac{v_x}{v_z},\ \alpha = \mathrm{atan}\ \frac{v_x}{v_z}$$

- Near the X-line, nongyrotropic pressure component $P^{(0)}_{yz} \sim m_e n v_y v_z$
- Electron pressure at the top/bottom EDR edge is gyrotropic: $P_{xy} \sim (P_{||} - P_{perp}) b_x b_y$ and changes linearly with y
- $P_{||}$, $P_{perp}$ are well approximated by either with CGL invariants or Egedal's theory

# Summary/Discussion

- ‘Real’ EDR: meandering

$P_{yz}$

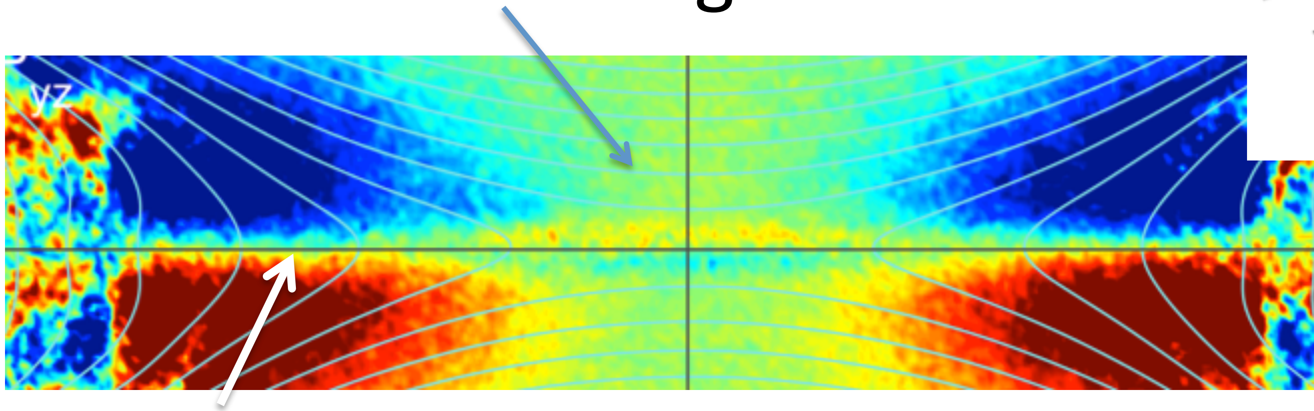

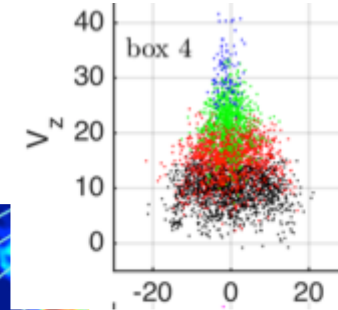


$V_z$

$V_x$

- ‘Extended’ EDR: $P_{yz}$ is due to electron anisotropy at inflow EDR edge
- The more inflowing electrons are anisotropic, the larger can be the extended EDR.
- Tasks to do next: compare to simulation results, eEDR scaling, etc…

# Thank you!